

Three-Dimensional Monolayers: Nanometer-Sized Electrodes of Alkanethiolate-Stabilized Gold Cluster Molecules

Stephen J. Green, Jennifer J. Stokes, Michael J. Hostetler, Jeremy Pietron, and Royce W. Murray*

Kenan Laboratories of Chemistry, University of North Carolina, Chapel Hill, North Carolina 27599-3290

Received: August 30, 1996[®]; In Final Form: October 23, 1996

Rotated disk electrode voltammetry is described for CH_2Cl_2 solutions of cluster molecules with nanometer-sized gold cores and stabilizing ligand shells consisting of mixed monolayers of octanethiolate and ω -ferrocenyloctanethiolate ligands in molar ratios ranging from 2:1 to 24:1. Voltammograms for the cluster molecules exhibit a ferrocene oxidation wave with a limiting current that is under hydrodynamic mass transport control. The current–potential curves preceding (“prewave”) and following (“postwave”) the ferrocene wave, which are ideally flat, are decidedly sloped. The $\Delta i/\Delta E$ slopes are proportional to the square root of electrode rotation rate, *i.e.*, are also under hydrodynamic control. The $\Delta i/\Delta E$ slopes are due to the charging of the electrical double layers of the cluster molecules, showing them to act as diffusing, molecule-sized “nanoelectrodes”. A theoretical analysis is presented of the transport control of the double layer charging. Possible reasons that the values of the cluster molecule capacitance (per unit surface area of cluster molecule, which entails use of models for the shape of the Au core of the cluster) are somewhat larger than the literature expectation for octanethiolate monolayers on flat gold surfaces are discussed. The tiny capacitances of the cluster molecules means that changing their charges by small potential increments can require an average of less than a single electron per cluster molecule.

Introduction

Following the initial report by Brust *et al.*¹ on a synthesis of gold clusters stabilized by monolayers of alkanethiolate ligands, we recently described² a further characterization of these nanometer-sized molecules and a route³ to mixed monolayers of alkanethiolate and ω -substituted alkanethiolate ligands on gold clusters. The reaction conditions of Brust *et al.*¹ produce, according to small angle X-ray scattering (SAXS) data⁴ on dodecanethiolate-stabilized cluster samples, gold cores with radii of 11.8–14.1 Å which can be taken as representing a dispersion of core sizes or as the short- and long-axis dimensions of the core shape, or both. The alkanethiolate ligands comprise 19.7 wt % of clusters prepared using octanethiol, according to thermogravimetric results.² Mixed monolayer clusters can be synthesized³ by solution place-exchange reactions between alkanethiolates on the cluster molecules and ω -substituted alkanethiols. According to ¹H NMR spectroscopy on mixed clusters prepared to date,³ as many as one-third of the original alkanethiolates can be place-exchanged with ω -ferrocenylalkane-thiolate ligands. The mixed clusters thus contain multiple equivalents of redox sites per cluster molecule, and voltammetric results³ for the ferrocenated clusters show that all are electrochemically reactive.

These cluster molecules have two essential components: the core-stabilizing alkanethiolate ligand monolayer and the Au core itself. We refer^{2,3} to the former component in terms of three-dimensional monolayers (3D-SAM), inasmuch as the alkanethiolate ligands can be investigated as bulk solid or solution samples and because they are confined upon molecule-sized spatial elements. In the solid state, FTIR results⁵ show that there are many structural similarities (and some differences) between 3D-SAMs and alkanethiolate monolayers on planar Au-(111) surfaces⁶ (2D-SAMs).

In this paper, we focus on the other cluster component, namely, the Au core, under the hypothesis that being a small metal particle, it will exhibit in an electrolyte solution the capacitive charging property that is well-known on planar electrode surfaces (*i.e.*, double layer charging). We have given³ a preliminary description of how this charging phenomenon is detected and here elaborate on that and give the relevant transport theory for its analysis. The charging of the cluster molecules' cores at a solid electrode/solution interface appears as a *mass transport controlled double layer charging*, which is an unusual electrochemical phenomenon.

The results will show that the area-normalized double layer capacitances of the cluster molecules bearing octanethiolate 3D-SAMs are quite small and are reasonably consistent with those of analogous 2D-SAM monolayers formed on Au surfaces with alkanethiolates.^{7–9} The capacitances, which we detect and measure using voltammetry, are strictly *electronic* in nature. The cluster double layer charging occurs independently of whether the cluster bears a redox group, but since the diffusion coefficient must be known to calculate the capacitance, we use a mixed monolayer, ferrocenated cluster in the experiments described. The mixed monolayer contains a mixture of octanethiolate and ω -substituted ferrocene octanethiolate ligands, and the voltammetric experiments are conducted in dichloromethane.

Experimental Section

Chemicals. Tetrabutylammonium perchlorate, Bu_4NClO_4 (Fluka, >99%) was dried under vacuum at 80 °C. Ferrocene (Aldrich, 97%) was resublimed. Dichloromethane, CH_2Cl_2 (Mallinckrodt, 99.9%), was dried over 4 Å molecular sieves. Acetonitrile, CH_3CN (Fisher, 99.9%), was redistilled from CaH_2 . ω -Substituted ferrocenyloctanethiol was exchanged into octanethiolate-stabilized gold clusters as previously described,³ to produce cluster compounds with ferrocenyloctanethiol:octanethiol molar ratios (abbreviated as $\text{C}_8\text{Fc}:\text{C}_8$) of 1:2, 1:5.5, 1:9.5,

[®] Abstract published in *Advance ACS Abstracts*, March 1, 1997.

and 1:24. These ratios were calculated from integration of the peaks corresponding to the ferrocene and methyl protons in the proton ^1H NMR spectra of the cluster compounds.

Electrochemical Measurements. Cyclic voltammetric data were acquired with a locally constructed potentiostat, with the potential waveform and the current signals (converted to voltage by the potentiostat) digitized by a DATEL-412 analog IO board in an IBM compatible PC using locally written software. Microelectrode voltammetry was performed using a microelectrode cell assembly described elsewhere,¹⁰ with the microdisk electrode being the tip of a 25 mm diameter Pt wire. The microelectrode was polished before use with a succession of alumina suspensions, finishing with 0.05 mm alumina (Buehler), which was also used to clean the electrodes between measurements. Polishing was always followed by extensive rinsing with water (Barnstead Nanopure, $>18\text{ M}\Omega/\text{cm}^2$).

Rotated disk electrode voltammetry was performed using an MSR rotator with a 0.15 cm^2 diameter glassy carbon electrode (Pine Instruments Co.) which was polished between experiments with 0.25 mm diamond polishing compound (Buehler) and rinsed with isopropyl alcohol and water (Barnstead Nanopure, $>18\text{ M}\Omega/\text{cm}^2$). The cell used had a working electrode compartment with a PTFE top with a flanged aperture for the working electrode; a rubber o-ring on the rotator shaft that gently butted against the PTFE flange gave free rotation with minimal evaporation of the volatile dichloromethane solvent. A Pt counter electrode and an SSCE reference electrode occupied the fritted side arms of the cell. The rotation rate dependence data reported are with rotated disk rates of 400, 625, 900, 1600, 2500, and 3600 rpm and a direct current (dc) potential sweep rate of 10 mV/s.

Cluster electrochemistry measurements were in 0.1 M $\text{Bu}_4\text{NClO}_4/\text{CH}_2\text{Cl}_2$ and control measurements of ferrocene electrochemistry were in 0.1 M $\text{Bu}_4\text{NClO}_4/\text{CH}_3\text{CN}$, with deoxygenation by solvent-saturated N_2 .

Results and Discussion

Currents obtained at rotated disk and microdisk electrodes in solvents free of Faradaic impurities and at potentials remote from "background" limits are, at sufficiently slow dc potential sweep rates, typically very small and potential-independent. Figure 1a shows a voltammogram obtained at a glassy carbon rotating disk electrode in a 0.1 mM solution of ferrocene in $\text{CH}_3\text{CN}/0.1\text{ M Bu}_4\text{NClO}_4$, and Figure 1c (inset) shows a similar experiment at a Pt microdisk electrode. In both cases, the slopes of the current–potential curves in the potential regions more negative ("prewave") and more positive ("postwave") than the ferrocene oxidation wave are small (*i.e.*, the background current is "flat").

The results with ferrocene solutions can be contrasted with those obtained, using the *same* electrodes, in consecutively performed measurements, with ferrocenes bound to the cluster molecules in a mixed monolayer. Parts b and d of Figure (inset) show results from *ca.* 1 μM solutions of a 1:5.5 $\text{C}_8\text{Fc}/\text{C}_8$ gold cluster compound in $\text{CH}_2\text{Cl}_2/0.1\text{ M Bu}_4\text{NClO}_4$. The ferrocenated cluster solutions exhibit a wave for oxidation of ferrocene.¹¹ (The "envelope" from positive and negative potential sweeps in Figure 1b appears larger than that for Figure 1a simply due to the difference in current scales. The same comment applies to Figure 1c,d of the inset.) The current–potential traces obtained in the cluster solutions are noticeably sloped (*i.e.*, currents are potential-dependent) in both the prewave and postwave potential regions. Such sloping regions in rotated and microdisk electrode work are commonly associated with imperfections in the working electrode and with effects

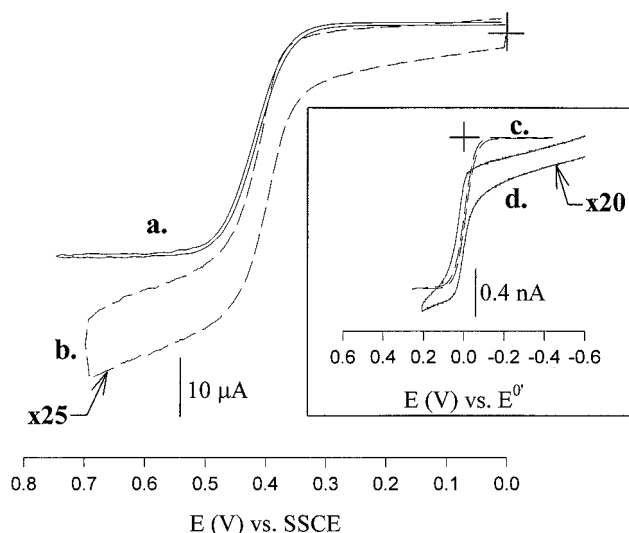


Figure 1. Voltammograms recorded at 25 mV/s at (curve a) a 0.15 cm^2 glassy carbon rotating disk electrode (3600 rpm) in 0.1 mM ferrocene in $\text{CH}_3\text{CN}/0.1\text{ M Bu}_4\text{NClO}_4$ and (curve b, current scale $\times 25$) in *ca.* 1 mM 1:5.5 $\text{C}_8\text{Fc}/\text{C}_8$ gold cluster compound in $\text{CH}_2\text{Cl}_2/0.1\text{ M Bu}_4\text{NClO}_4$. The figure inset shows the result of these two experiments (curves c, d, respectively) at a 25 mm Pt microelectrode at 10 mV/s (current scale $\times 20$ for curve d).

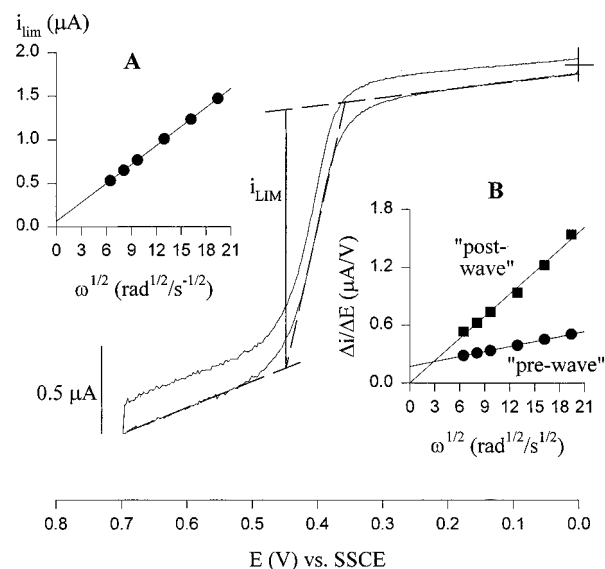


Figure 2. Voltammogram recorded at 10 mV/s at a 0.15 cm^2 glassy carbon rotating disk electrode (3600 rpm) in *ca.* 1 mM 1:5.5 $\text{C}_8\text{Fc}/\text{C}_8$ gold cluster compound in $\text{CH}_2\text{Cl}_2/0.1\text{ M Bu}_4\text{NClO}_4$. Inset A shows the dependence of the limiting current for this voltammetry on the square root of the electrode rotation rate ($\omega^{1/2}$), while inset B shows the dependence on $\omega^{1/2}$ of the prewave and postwave slopes of the voltammetry.

of uncompensated solution resistance. However, since, on comparable current scales, the current–potential slopes are greater than in blank solutions or in experiments on monomeric ferrocene solutions with the same electrodes, the slopes must be a real phenomenon associated with the use of cluster molecules with gold cores. The phenomenon is in fact associated with the double layer capacitances of individual cluster molecules that are mass transported to the working electrode surface and there become charged to the potential applied to the working electrode.

Figure 2, center, shows another rotated disk voltammogram of a *ca.* 1 mM solution of the 1:5.5 $\text{C}_8\text{Fc}/\text{C}_8$ gold cluster compound. The sloping prewave and postwave regions in the current–potential curve are again observed. The slope of the

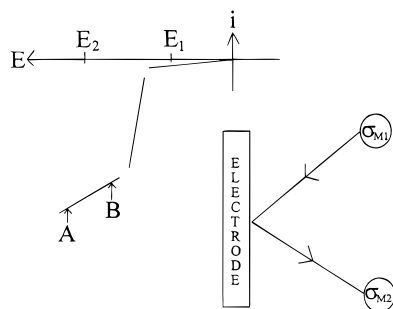


Figure 3. Stylized rotating disk voltammogram for the ferrocenated clusters. The inset shows schematically the charging of the cluster core from a charge per unit core surface area of σ_{M1} at potential E_1 (in solution) to one of σ_{M2} at potential E_2 (the electrode potential). A and B indicate different “ E_2 ” values used in deriving eq 8 for the cluster double layer capacitance $C_{DL,CLUSTER}$.

postwave region is consistently greater than that of the prewave current–potential region. Measuring limiting currents for the voltammogram (as shown) at a series of electrode rotation rates, we find that (Figure 2, inset A) the limiting current of the ferrocene oxidation wave varies with the square root of the rotation rate ($\omega^{1/2}$), which is a diagnostic¹² for the mass transport of the cluster molecules to the electrode surface being under hydrodynamic control. That the slopes $\Delta i/\Delta E$ of the prewave and postwave regions are also proportional to $\omega^{1/2}$ (Figure 2, inset B) demonstrates that the double layer charging of the clusters is under hydrodynamic mass transport control. (It should be noted that current associated with charging the double layer of the rotated electrode itself is insensitive to electrode rotation.) The theoretical analysis given below will support the Figure 2 analysis. Stated differently, since an electron flow associated with the charging of the double layer of the metal-like cluster core can be voltammetrically characterized as transport-controlled, the solvated clusters are demonstrated to be freely-diffusing “nanoelectrodes”.

The limiting currents at the rotated disk electrode (Figure 2, center) that arise from the Faradaic oxidation of the ferrocene groups on the clusters can be represented by the Levich equation¹²

$$i_{LIM} = 0.62FAD_{CLUSTER}^{2/3}\omega^{1/2}\nu^{-1/6}C_{CLUSTER}\theta_{Fc} \quad (1)$$

where $D_{CLUSTER}$ and $C_{CLUSTER}$ are the diffusion coefficient and concentration of cluster molecules, θ_{Fc} is the number of ferrocenes per cluster, A is the area of the rotated disk electrode, and the other symbols take their usual meaning.¹² On the basis of comparisons of $D_{CLUSTER}$ results obtained using eq 1 to those³ of non-electrochemically based diffusion measurements, we have shown³ that the voltammetric oxidation of the ferrocene cluster sites is quantitative, or nearly so, and that the ferrocenes react more or less independently of one another. Figure 3 shows a stylized rotated-disk voltammogram in a cluster solution, where the average charge on a cluster molecule in the solution from which mass transport occurs is given as σ_{M1} and its charge following its encounter with the electrode as σ_{M2} , assuming equilibration of the electrode and cluster core Fermi levels. Schematically, the cluster core is charged from σ_{M1} to σ_{M2} (σ_M = charge per unit core surface area) in moving from potential E_1 (its potential in the solution) to potential E_2 (that of the electrode). Inserting a term for this charging into eq 1 gives

$$i_{LIM} = 0.620AD_{CLUSTER}^{2/3}\omega^{1/2}\nu^{-1/6}C_{CLUSTER}[(\sigma_{M2} - \sigma_{M1})N_A A_{CLUSTER} + F\theta_{Fc}] \quad (2)$$

where N_A is Avogadro’s number, $A_{CLUSTER}$ is the area of the

cluster core, and i_{LIM} is now measured with respect to currents flowing at the rotated disk electrode in the absence of cluster solution.

Considering that the charge σ_{M2} that the cluster bears depends on the value of the potential E_2 , and that changing that potential from potential E_A to E_B changes the charge on cluster molecule following encounter with the electrode from σ_{MA} to σ_{MB} , the currents flowing at potentials E_A and E_B can be expressed respectively as

$$i_A = 0.62AD_{CLUSTER}^{2/3}\omega^{1/2}\nu^{-1/6}C_{CLUSTER}[(\sigma_{MA} - \sigma_{M1})N_A A_{CLUSTER} + F\theta_{Fc}] \quad (3)$$

$$i_B = 0.62AD_{CLUSTER}^{2/3}\omega^{1/2}\nu^{-1/6}C_{CLUSTER}[(\sigma_{MB} - \sigma_{M1})N_A A_{CLUSTER} + F\theta_{Fc}] \quad (4)$$

The difference Δi between these currents is

$$\Delta i = i_A - i_B = 0.62AD_{CLUSTER}^{2/3}\omega^{1/2}\nu^{-1/6}C_{CLUSTER}(\sigma_{MA} - \sigma_{MB})N_A A_{CLUSTER} \quad (5)$$

and division by $\Delta E = E_A - E_B$ gives

$$(i_A - i_B)/(E_A - E_B) = \Delta i/\Delta E = 0.62AD_{CLUSTER}^{2/3}\omega^{1/2}\nu^{-1/6}C_{CLUSTER}[(\sigma_{MA} - \sigma_{MB})N_A A_{CLUSTER}/(E_A - E_B)] \quad (6)$$

where $\Delta i/\Delta E$ is recognized as the postwave slope of the current–potential curves in Figures 1 and 2 and

$$(\sigma_{MA} - \sigma_{MB})/(E_A - E_B) = C_{DL,CLUSTER} \quad (7)$$

where $C_{DL,CLUSTER}$ is the double layer capacitance of the metal core in F/cm² which is proportional to $\Delta i/\Delta E$.

Combining 6 and 7 gives

$$C_{DL,CLUSTER} = (\Delta i/\Delta E)/[0.620AD_{CLUSTER}^{2/3}\omega^{1/2}\nu^{-1/6}C_{CLUSTER}N_A A_{CLUSTER}] \quad (8)$$

Equation 8 shows that the slopes of plots of $\Delta i/\Delta E$ vs $\omega^{1/2}$, such as that in Figure 2, inset B, can be used to calculate double-layer capacitances for the clusters, providing that $C_{CLUSTER}$, $D_{CLUSTER}$, and $A_{CLUSTER}$ are known. Equation 8 can be applied to both the prewave and postwave potential regions.¹³ Calculation of $C_{DL,CLUSTER}$ involves some assumptions about the shape of the Au core of the cluster, as outlined next.

While the gold core dimension (11.8–14.1 Å, by SAXS) and the weight fraction of alkanethiolate ligand (19.7%, by thermogravimetry) of the octanethiolate cluster samples are known, the gold core shape (and equivalently the cluster molecular weight) has to be assumed. The early report by Brust *et al.*¹ suggested a cuboctohedral shape from HRTEM images, and in our subsequent reports^{2,3} we used this as the model shape for purposes of calculating various cluster parameters. Completed cuboctahedra would contain 55, 147, 309, 561, etc., Au atoms. Recent reports by Whetten *et al.*¹⁴ and Luedtke and Landman¹⁵ present evidence, however, that the alkanethiolated gold clusters have a polyhedral morphology of truncated octahedra and give mass spectral data consistent with core sizes of 116, 140, 225, 314, and 459 atoms. The shape analysis of these clusters is clearly an evolving subject, and thus we will analyze the cluster capacitance results in terms of both assumed shapes. Cuboctahedra of 309 and 561 gold atoms (taking the Au–Au bond

TABLE 1: Results of Diffusion Coefficients and Double Layer Capacitances for Ferrocenated Cluster Molecules

C ₈ Fc/C ₈ ^a	no. of runs	D_{CLUSTER}^b (cm ² /s)	$(C_{\text{DL,CLUSTER}} \times A_{\text{CLUSTER}})/$ MW _{CLUSTER} (F mol/g)		ratio of postwave to prewave $C_{\text{DL,CLUSTER}}$	309 atom cuboctahedron model			314 atom truncated octahedron model		
			prewave	postwave		θ_{Fc}^c	$C_{\text{DL,CLUSTER}}^d$ (F/cm ²)		θ_{Fc}^e	$C_{\text{DL,CLUSTER}}^f$ (F/cm ²)	
							prewave	postwave		prewave	postwave
1:2	1	3.6×10^{-6}	7.3×10^{-24}	5.8×10^{-23}	7.9	34	3.1×10^{-6}	2.4×10^{-5}	35	2.4×10^{-6}	1.9×10^{-5}
1:5.5	4	2.8×10^{-6}	6.2×10^{-24}	3.5×10^{-23}	5.7	16	2.5×10^{-6}	1.4×10^{-5}	16	1.9×10^{-6}	1.1×10^{-5}
1:9.5	2	$(\pm 11\%)$	$(\pm 25\%)$	$(\pm 36\%)$	3.4	10	$(\pm 25\%)$	$(\pm 36\%)$	10	$(\pm 25\%)$	$(\pm 36\%)$
		2.7×10^{-6}	7.1×10^{-24}	2.4×10^{-23}			2.8×10^{-6}	9.6×10^{-6}		2.2×10^{-6}	7.5×10^{-6}
1:24	1	$(\pm 4\%)$	$(\pm 3\%)$	$(\pm 10\%)$	3.4	4	$(\pm 3\%)$	$(\pm 10\%)$	4	$(\pm 3\%)$	$(\pm 10\%)$
		2.6×10^{-6}	8.9×10^{-24}	3.0×10^{-23}			3.5×10^{-6}	1.2×10^{-5}		2.7×10^{-6}	9.2×10^{-6}

^a By NMR; the relation numbers of terminal ferrocene to methyl groups, average, on a cluster molecule. ^b From application of eq 1 to i_{LIM} results. ^c Multiplying by 1.82 converts 309 model results to 561 model results. ^d Multiplying by 1.26 converts 309 model results to 561 model results. ^e Multiplying by 1.46 converts 314 model results to 459 model results. ^f Multiplying by 1.18 converts 314 model results to 459 model results.

distance in Au metal, 2.88 Å) have theoretical “short” and “long” axes of 9–11 Å (309 Au atoms), and 12–14 Å (561 Au atoms), so both have sizes consistent with the SAXS results. According to the thermogravimetric analysis, these cuboctahedra would be covered with *ca.* 103 or 187, respectively, octanethiolate chains attached to the 162 and 252 surface Au atoms. Truncated octahedra containing¹⁴ 314 or 459 gold atoms would have 174 or 234 surface atoms, respectively, a somewhat wider spread of long- and short-axis dimensions compared with the cuboctahedra, and 105 or 153 attached octanethiolate chains, respectively. We will present the capacitance results in terms of 309 and 561 atom cuboctahedra, and 314 and 459 atom truncated octahedra, as *models* of the cluster core shape. The modest uncertainties that result do not affect the case for the double layer charging phenomenon but are part of the comparison of the numerical values of surface-area-normalized cluster capacitances to those of 2D-SAMs.

It is worth delineating which cluster parameters are shape-dependent; they include the monolayer coverage (number of alkanethiolate ligands per Au atoms on the core surface), the surface area of the cluster core, the number of ferrocenes attached to mixed monolayer clusters, and the molecular weight. Measurements of the diffusion coefficients of ferrocenated clusters using limiting currents as in Figure 2 and eq 1, however, do not depend on assumptions regarding the core shape, since eq 1 contains the product $C_{\text{CLUSTER}}\theta_{\text{Fc}}$.

From the ¹H NMR spectra of the ferrocenated clusters, the ratio of ferrocene sites to octanethiolate methyl end groups was calculated, and these data are given in Table 1 (C₈Fc:C₈) for the mixed monolayer cluster samples studied, as are the diffusion coefficient measurements for the various preparations. Except for the highest loading, the D_{CLUSTER} results are consistent with those in our previous, preliminary report.³ Application of the D_{CLUSTER} results and eq 8 to the slopes of plots of $\Delta i/\Delta E$ vs. $\omega^{1/2}$ leads, after normalization for cluster concentration expressed as grams per liter, to results for the product $A_{\text{CLUSTER}}C_{\text{DL,CLUSTER}}/\text{MW}_{\text{CLUSTER}}$ given in Table 1.¹⁶ This product and the ratio of postwave to prewave $C_{\text{DL,CLUSTER}}$, also given in Table 1, contain no assumptions regarding the gold core shape. Further analysis of the data requires such assumption. Taking the 309 atom cuboctahedral and 314 atom truncated octahedral models, Table 1 shows the values of $C_{\text{DL,CLUSTER}}$ (both prewave and postwave) and the number θ_{Fc} of ferrocenyl groups per cluster molecule obtained for the two models. $C_{\text{DL,CLUSTER}}$ (F/cm²) is a capacitance that has been normalized for the surface area of the gold core which is 1.96×10^{-13} and 2.55×10^{-13} cm² for the 309 and 314 atom models, respectively.

The results given in Table 1 confirm that although the calculated value of $C_{\text{DL,CLUSTER}}$ is model-dependent, the effect of the choice of model is not dramatic. The greatest difference is between the 314 atom truncated octahedron and the 561 atom

cuboctahedron results, which still only differ by a factor of 1.6. With this qualification in mind, it is interesting to compare the results in Table 1 with existing data for the double layer capacitance of self-assembled alkanethiol monolayers on gold electrodes in aqueous electrolytes,^{7–9} which we note generally yield slightly higher double layer capacitances at bare metal electrodes than nonaqueous electrolytes such as that used in our study.¹⁷

In the prewave region, the ferrocenated clusters can be considered as an approximate analogy¹⁸ to purely octanethiol-stabilized clusters, since previous studies on two-dimensional alkanethiol monolayers on gold electrodes^{8,9} report a relatively weak dependence of capacitance on end group, and the ferrocene alkanethiols on the lower three cluster samples are diluted by at least 5.5-fold. Certainly, from Table 1, the prewave capacitance shows no trend with θ_{Fc} , though the random errors in the experiment are rather large and any subtle trend would be obscured.

Porter *et al.*⁷ used cyclic voltammetry to measure the double layer capacitance of self-assembled monolayers of *n*-alkanethiols (from *n* = 1 to *n* = 21) on polycrystalline gold electrodes in water, as functions of potential scan rate and electrolyte. With ClO₄[−], (the anion used in our study), the double layer behaved as an “ideal” capacitor (as in the Helmholtz model of the double layer¹²) at *n* ≥ 9, and for shorter chains an increasing relative dielectric constant (normalized for monolayer thickness) indicated penetration of ClO₄[−] into the monolayer. Interpolation of his data⁷ at *n* = 8, where this effect of ion penetration was only slight, suggests a capacitance at 100 mV/s¹⁹ of around 1.9×10^{-6} F/cm². This value is remarkably close to the prewave capacitances given in Table 1 for octanethiol-/ferrocenyloctanethiol-stabilized clusters. The prewave cluster capacitances are, however, somewhat larger.

Considering the preceding analogy, it is worth discussing why the double layer capacitance of a flat, octanethiol-coated electrode (a “two-dimensional” monolayer) might differ from that of an octanethiol-coated cluster (a “three-dimensional” monolayer). Specifically, differences may arise from the different capacitor geometries and from any differences in the structure of the monolayers.

First, if we treat the cluster as a sphere, and both capacitors as ideal, which is a reasonable approximation from existing monolayer capacitance studies,^{7–9} then the capacitances per unit area (of metal) are

$$C = \epsilon_r \epsilon_0 / d \quad (9)$$

for the two-dimensional case, where *C* is the capacitance per unit area, ϵ_r is the relative dielectric of the monolayer, ϵ_0 is the permittivity of free space, and *d* is the monolayer thickness, and

$$C = [\epsilon_r \epsilon_0 / d] [(a + d)/a] \quad (10)$$

for the three-dimensional case, where a is the gold core radius. From eqs 9 and 10, we conclude that, for the octanethiol-stabilized clusters considered here, since the values of a and d are similar (the length of an extended C_8 chain is *ca.* 10 Å), the geometric capacitance should be about twice that of a similarly coated flat electrode.

Second, in comparing monolayer structures, important points are the packing arrangement of the chains, which will govern the monolayer thickness, and the presence of any defects in the monolayers. Since no detailed data are available on the packing of the chains on cluster molecules in solutions, we are limited to the estimation that, were the equivalent monolayer to be tightly packed on the cluster, it would be thinner on a curved compared with a flat surface. In this case, the capacitance per unit area for the clusters would be larger than that of two-dimensional monolayers.

Concerning the presence of defects in the monolayers, FTIR studies of clusters as solid suspensions in KBr show a significant population of end-gauche defects, whereas there is no evidence for such defects in two-dimensional monolayers.⁵ There is, however, no equivalent evidence for the solution state clusters, and extrapolating the FTIR conclusions to the solution state would be speculative. To the extent that defects might be present, however, the cluster capacitance would be increased, since defects allow ions to penetrate the monolayer and increase its relative dielectric.

Thus, from all of the above considerations we would expect the cluster molecules to have a somewhat larger double layer capacitance (in the prewave region) than that of an octanethiol-coated flat gold electrode. In comparison with the 1.9×10^{-6} F/cm² result of Porter *et al.*,⁷ this would appear to be the case.

Examining the postwave capacitance results in Table 1, it is immediately apparent that oxidizing the ferrocenyl groups sharply increases the cluster capacitance (by close to 8-fold for the 1:5.5 cluster). Indeed, from the ratio of postwave to prewave capacitances, it is evident that the larger the θ_{Fc} , the greater the increase in capacitance. This result is entirely expected, since the effect of the ferricinium groups would be analogous to the adsorption of ions on a metal electrode, which also increases double layer capacitance.¹⁷ It is perhaps surprising that there is no trend with θ_{Fc} in the values of postwave capacitance. However, the random error in the measurements is even larger than in the prewave results.

Evidently, using a solid electrode, we may influence the double layer of the cluster both electronically, by changing the electron population of the core through its electrical contact (via its alkanethiolate skin) with the electrode, and, ionically, by changing the redox state of the attached ferrocenyl groups. The electronic capacitances of the cluster molecule nanoelectrodes means that, even without the presence of redox groups in their monolayers, the clusters can be considered to be electron donors and acceptors in chemical reactions.

In conclusion, it is clear from these studies that we are able to observe the charging of the double-layer capacitance of a freely-diffusing gold cluster compound, which can thus be treated as a molecule-sized electrode, or nanoelectrode. Capacitance studies have in the past been used to learn about the structure of alkanethiolate monolayer assemblies on flat electrodes,⁷⁻⁹ and we are now poised to extend such studies to the three-dimensional monolayers of gold cluster compounds. Preliminary data²⁰ show that the cluster capacitance increases with decreasing alkane chain length. Other accessible experiments explore the effects of the end groups on the alkanethiolate,

of the electrolyte and its concentration, and of a change in the gold core size, which is controllable through the conditions of the cluster preparation.²¹

As a final point, it is interesting to note a potentially important consequence of the extremely small size of the cluster molecules, considered as distributed nanoelectrodes. The surface area of the gold core is of the order $\sim 10^{-13}$ cm² and the capacitance per individual nanoelectrode is of the order $\sim 10^{-19}$ F. From the relation $C = Q/V$, where C is capacitance, Q is charge, and V is voltage, the tiny nanoelectrode capacitance means that a potential change of some tenths of a volt is necessary to add a single electron to the double layer of a single cluster molecule. For smaller voltage changes one is forced to conclude that some cluster-electrode collisions result in charging by a single electron and some do not, in a probabalistic fashion. Stated differently, in the cluster solution, for a given average charge (σ), at equilibrium there will be a distribution of the charge on individual cluster molecules that will range over a few units of electron charge. The charging of clusters at electrodes by an average of less than one electron in effect just shifts the maximum of the charge distribution profile.

The preceding result is certainly unusual, but one can consider an analogous situation for an array of small microdisk electrodes. For a 1 μ m microdisk radius and a double layer capacitance of 10 μ F/cm², changing the microelectrode's potential by 2.5×10^{-7} V would result in passage, on average, of 0.5 electron per microdisk.

Acknowledgment. This research was funded in part by grants from the National Science Foundation and the Office of Naval Research.

References and Notes

- (1) Brust, M.; Walker, M.; Bethell, D.; Schiffrin, D. J.; Whyman, R. *J. Chem. Soc., Chem. Commun.* **1994**, 801-802.
- (2) Terrill, R. H.; Postlethwaite, T. A.; Chen, C.-H.; Poon, C. D.; Terzis, A.; Chen, A.; Hutchison, J. E.; Clark, M. R.; Wignall, G.; Londono, J. D.; Superfine, D.; Falvo, M.; Johnson, C. S.; Samulski, E. T.; Murray, R. W. *J. Am. Chem. Soc.* **1995**, *117*, 12537-12548.
- (3) Hostetler, M. J.; Green, S. J.; Stokes, J. J.; Murray, R. W. *J. Am. Chem. Soc.* **1996**, *118*, 4212-4213.
- (4) Londono, J. D.; Hostetler, M. J.; Murray, R. W. Unpublished results.
- (5) Hostetler, M. J.; Stokes, J. J.; Murray, R. W. *Langmuir* **1996**, *12*, 3604-3612.
- (6) (a) Dubois, L. H.; Nuzzo, R. G. *Annu. Rev. Phys. Chem.* **1992**, *43*, 437-463. (b) Ulman, A. *An Introduction to Ultrathin Organic Films*, Academic: New York, 1991. (c) Bain, C. D.; Whitesides, G. M. *Angew. Chem., Int. Ed. Engl.* **1989**, *28*, 506-512.
- (7) Porter, M. D.; Bright, T. B.; Allara, D. L.; Chidsey, C. E. D. *J. Am. Chem. Soc.* **1987**, *109*, 3559-3568.
- (8) Chidsey, C. E. D.; Loiacono, D. N. *Langmuir* **1990**, *6*, 682-691.
- (9) Sondag-Huethorst, J. A. M.; Fokink, L. G. J. *Langmuir* **1995**, *11*, 2237-2241.
- (10) Watanabe, M.; Wooster, T. T.; Murray, R. W. *J. Phys. Chem.* **1991**, *95*, 4573-4579.
- (11) We have firm evidence from ¹H NMR that solutions of ferrocenated cluster compounds contain no dissociated ferrocenyloctanethiol or -thiolate. The voltammetric ferrocene wave is due solely to ferrocene sites bound to the cluster molecules.
- (12) Bard, A. J.; Faulkner, L. R. *Electrochemical Methods*; Wiley: New York, 1980; pp 288, 500.
- (13) The plot of $\Delta i/\Delta E$ vs $\omega^{1/2}$ for the prewave potential region in Figure 2, inset B, has an intercept, which is not predicted by eq 8, that is thought to arise from lack of correction of the very small currents in the prewave potential region for the background currents which flow as a result of capacitive charging at the disk electrode alone. Applying a correction is complicated by the fact that the clusters tend to adsorb on the working electrode; such adsorption is in principle of no consequence for steady state currents, but it does mean that a correction derived from a naked electrode background current is strictly speaking inexact.
- (14) Whetten, R. L.; Khoury, J. T.; Alvarez, M. M.; Murthy, S.; Vezmar, I.; Wang, Z. L.; Stephens, P. W.; Cleveland, C. L.; Luedtke, W. D.; Landman, U. *Adv. Mater.* **1996**, *8*, 428-433.
- (15) Luedtke, W. D.; Landman, U. *J. Phys. Chem.* **1996**, *100*, 13323-13329.

(16) Application of eq 1 and i_{LIM} values measured as shown in Figure 2 assumes that the i_{LIM} measurement itself does not include any cluster molecule charging current. This is an approximation since the extrapolation method for measuring i_{LIM} depicted in Figure 2 presumes a constant cluster double layer capacitance whereas in fact the postwave slope is obviously larger than the prewave slope. This effect could lead to an overestimation of the cluster diffusion coefficient and an underestimation of $C_{\text{DL,CLUSTER}}$. However, the obtained D_{CLUSTER} values are compatible with other non-electrochemical measurements³ and also lead to hydrodynamic radii that are physically reasonable, which indicates that the i_{LIM} measurement approximation is not a serious one. Nonetheless we continue to probe the proper measurement of experimental i_{LIM} .

(17) Delahay, P. *Double Layer and Electrode Kinetics*; Interscience: New York, 1965.

(18) (a) The ferrocenated clusters are not good analogies to the ferrocenated 2D-SAMs described by Shimazu et al.^{18b} Those ferrocenyl-

undecanethiolate monolayers were not diluted by unsubstituted alkanethiolate and are thus somewhat disorganized⁷ by steric interactions between the bulky ferrocene sites, allowing solvent and ion penetration and exhibiting substantially enhanced double layer capacitances ($20 \times 10^{-6} \mu\text{F}/\text{cm}^2$). (b) Shimazu, K.; Ye, S.; Sato, Y.; Uosaki, K. *J. Electroanal. Chem.* **1994**, 375, 409.

(19) A value of 100 mV/s was the fastest scan rate used by Porter *et al.*,⁷ and is felt to be the most appropriate in any comparison to the cluster charging case, since we assume that the clusters are charged "instantly" when they reach the electrode. Porter *et al.*⁷ noted that, in cases where ions were believed to penetrate the monolayer, capacitance was an increasing function of decreasing scan rate (*i.e.*, greater time allows greater ion penetration).

(20) Wuelfing, P.; Green, S. J.; Hostetler, M. J.; Murray, R. W. Unpublished results.

(21) Hostetler, M. J.; Murray, R. W. Unpublished results.